

# PROCEEDINGS OF SPIE

[SPIDigitalLibrary.org/conference-proceedings-of-spie](https://spiedigitallibrary.org/conference-proceedings-of-spie)

## Fabrication of IC-compatible capacitive sensors by polymer processing

Pedersen, Michael, Olthuis, Wouter, Bergveld, Piet

Michael Pedersen, Wouter Olthuis, Piet Bergveld, "Fabrication of IC-compatible capacitive sensors by polymer processing," Proc. SPIE 3046, Smart Structures and Materials 1997: Smart Electronics and MEMS, (19 June 1997); doi: 10.1117/12.276630

**SPIE.**

Event: Smart Structures and Materials '97, 1997, San Diego, CA, United States

# Fabrication of IC-compatible capacitive sensors by polymer processing

Michael Pedersen, Wouter Olthuis, and Piet Bergveld

MESA Research Institute, University of Twente, P.O. Box 217,  
NL-7500 AE Enschede, the Netherlands<sup>#</sup>

## ABSTRACT

A low-temperature (<300 °C) polymer micromachining process has been developed, whereby the sensor can be fabricated directly on substrates containing complete electronic circuits. This approach is strong since any IC process can be selected with no regard to the sensor process. Condenser microphones have been fabricated with a sensitivity of 8.1 mV/Pa, flat frequency response between 100 Hz and 15 kHz, and an equivalent noise level of 24 dBA SPL. Differential pressure sensors have been made with a nominal sensitivity  $\Delta C/C$  of 17 %/bar for a pressure range 1 bar. Furthermore, uni-axial accelerometers with a nominal sensitivity of 0.43 %/g have been implemented. From these results it may be concluded that IC-compatible capacitive sensors with good performances can be achieved with this technology, and it is suggested that the use of polymer processing on silicon therefore may become an important issue in smart sensors of the future.

**Keywords:** silicon sensors, integrated sensors, capacitive sensors, polymer processing, polyimide

## 1. INTRODUCTION

The development of smart systems and systems with adaptive properties is for a large part a problem associated with control engineering. However, in order to derive a precise and sufficient control strategy, detailed knowledge about the properties and the conditions within the system must be available. The sensor is therefore an essential part, which must provide the necessary information required to control the system. As a higher degree of precision and controllability of the system is required, so is the amount of information provided by the sensors. In most cases this leads to the conclusion that a higher distribution of sensors is necessary to provide adequate information.

In some cases, a higher distribution of conventional sensors is not feasible due to limitations of weight, size, and price. With the introduction of sensors made by silicon micromachining<sup>1</sup>, new possibilities for the miniaturisation of the measurement systems have emerged. The potential integration of sensors and signal detection circuits on the same silicon chip yields not only the greatest possible miniaturisation, but also a higher flexibility and simplification of the structure of the complete system, i.e. if a standard system (a bus) is used between the sensors and the rest of the system. Such integrated sensors, known as smart sensors<sup>2</sup>, are devices which not only detect a certain physical quantity, but also have the capabilities on board which can transform the signal into a standard form, thereby allowing a standard interface with the control system. This modular approach is of great value in any system, and the tiny integrated silicon sensors can provide new applications in systems with small dimensions, which have previously been difficult to control. Furthermore, the integrated silicon sensors have proven to be applicable in systems where size is not absolutely critical (e.g. airbag systems in cars)<sup>3</sup>, which is mainly due to the potential of fabrication of very large numbers of devices at a relatively low price, associated with the silicon technology. Additionally, there are sensing principles which performance/precision can be directly improved by integrating a signal detection circuit in close proximity. This is especially the case for capacitive sensors, where the parasitic capacitance of the interconnection between the sensor and the detection circuit can have great influence on the performance, and normally is the problem that obstructs the use of the otherwise superior capacitive sensors, regarding sensitivity and power consumption.

The integration of sensors and integrated circuits on one silicon chip may seem straight forward, since both parts are available on silicon. However, the discipline aims to bring together technologies, which have been developed on completely different backgrounds. The IC technology has developed into a well established technology with well known and controlled characteristics. This allows the designer to regard the components in the process as building blocks with certain properties,

---

<sup>#</sup> Further author information -

M.P.(correspondence): Email: M.Pedersen@eltn.utwente.nl; Telephone: +31-53-4892722; Fax: +31-53-4892287

W.O.: Email: W.Olthuis@eltn.utwente.nl; Telephone: +31-53-4892688

P.B.: Email: P.Bergveld@eltn.utwente.nl; Telephone: +31-53-4892720

whereas no exact knowledge of the fabrication technology is required. The micro electromechanical systems (MEMS) technology is very different on this point, as the designer is required to know the possibilities and limitations of the fabrication processes to find the best possible design. Moreover, the MEMS technology is a very "open" technology, where the application of many different structures and materials is possible, and can be exploited to achieve the best sensor performance. Bringing together the very strict IC technology and the "chaotic" MEMS technology therefore poses significant problems, especially since one wants to preserve the control of the very complex IC technology. This desire leads to the conclusion that if any sensor is to be made on a chip also containing integrated circuits, it must be carried out in a manner which will not in any way influence the performance of the integrated circuits. A derivative hereof is that in no way should the IC process be interfered with or interrupted, as this is certain to influence the device characteristics. Consequently, the sensor must be fabricated either by the IC process itself, or by a process which can be performed without affecting the integrity of the IC process. In principle a similar rule should apply that the performance of the sensor should not be influenced by the fabrication of an integrated circuit. Since any IC process contains very high temperature processes ( $>1000\text{ }^{\circ}\text{C}$ ), it is excluded that a sensor structure or parts of it may be present on the silicon substrate before IC processing, since the high temperatures will change the mechanical and/or electrical properties of the materials in the sensor. This leaves the option that the sensor is made on the silicon substrate after completion of the integrated circuits (post processing). The delicacy of the IC technology, however, leaves very few fabrication processes which are compatible. Firstly, the process temperature should be kept under  $350\text{--}400\text{ }^{\circ}\text{C}$ , to ensure the stability of the aluminium interconnection layers and to avoid exceeding the limit of mechanical stress which could cause damage, e.g. cracks, in the IC structures. Secondly, a number of low-temperature processes are known to influence IC devices, including e-beam evaporation<sup>4</sup>, plasma-enhanced chemical vapour deposition (PECVD), and RF sputtering<sup>5</sup>. Lastly, the etching of silicon with liquid chemicals, such as potassium hydroxide (KOH), requires that the IC structures are physically protected from the liquid, as it will instantly destroy the structure. Achieving this protection on 4", 6", or 8" substrates may prove very difficult, and wet chemical etching of silicon should therefore be avoided. In this paper we describe how the introduction of polymer processing can make the sensor process fully compatible with IC structures. Furthermore, it will be shown that the modular sensor process can be applied to the fabrication of numerous types of capacitive sensors, requiring only a modification of the photolithographic masks in the process, thereby also allowing the fabrication of different sensors on the one and same silicon substrate.

## 2. POLYIMIDE TECHNOLOGY APPLIED IN SILICON MICROMACHINING

Polymers are a group of materials which remain to be exploited in the micromachining technology. The major reasons for this are the well known problematic properties of most polymers, such as water absorption, chemical and thermal instabilities, and viscoelastic properties. However, from the processing point of view these materials are ideally suited for sensor processes to be integrated with IC processes, since the application and definition of such layers is very simple, and normally can be done with the same spin-on technology used for photoresist layers in lithographic processes. Considering the restrictions mentioned above, it is an interesting prospect to consider the use of polymers in an IC compatible sensor process. However, a polymer must be used, which has good chemical and mechanical properties, to withstand the other processing steps still required to create the complete sensor. Polyimide might be a suitable polymer for this purpose, and is a material which has already been investigated extensively and has found use as passivation and insulation layer in IC technology. In the following the most important properties for micromechanical parts of sensors made of this material will be discussed.

### 2.1 Polyimide chemistry and processing

Polyimide compounds are classified as cyclic-chain polymers. They are characterised by the presence of a so-called imide functionality, a cyclic amine bound to two of the carbonyl groups, surrounding the aliphatic or aromatic group in the main chain.

The basic procedure for the synthesis of polyimide is initiated by first forming a polyamic acid by a polycondensation reaction of an acid dianhydride and a difunctional base (diamine). The polyamic acid precursor formed by this reaction is soluble in polar inorganic solvents, such as n-methylpyrrolidone (NMP), dimethyl formamide (DMF) and dimethylsulfoxide (DMSO). The polyamic acid can subsequently be imidised by applying energy (heat), whereby the solvent is removed, and a chemical reaction (ring closure) is forced. During the ring closure, water is expelled from the molecular structure in an irreversible reaction, thereby forming the polyimide. This heat treatment, known as "curing", is typically carried out at a temperature ranging from  $300\text{ }^{\circ}\text{C}$  to  $500\text{ }^{\circ}\text{C}$ . The temperature required to imidise the polymer depends on the exact materials used for the synthesis. Since, the imidisation is irreversible the polyimide can in principle not absorb water, however, since these kinds of processes are statistical, perfect imidisation can never be obtained, wherefore sites always remain in the

polymer chains, where water molecules may be bound. The perfection of imidisation and the cross linking formed has direct influence on the polyimide properties, such as thermal, mechanical and electrical stability. For the commercialisation of these materials, numerous different polyamic acids have been developed, however, the most common and well documented synthesis is based on pyromellitic acid dianhydride (PMDA) and oxydianiline (ODA), forming a polyimide known from the duPont® Kapton® film<sup>6</sup>, which is widely used in packaging processes. The processing of polyimide in microtechnology makes use of the already well known spin-on technology, used for the resist in the photolithography. The resins used to form the polyimide films are typically solutions containing the polyamic acid precursor dissolved in one of the organic solvents mentioned above. Such polyimide resins based on different syntheses are commercially available from different suppliers, which include duPont® (PI), Hitachi (PIQ) and Ciba-Geigy (Probidimide™).

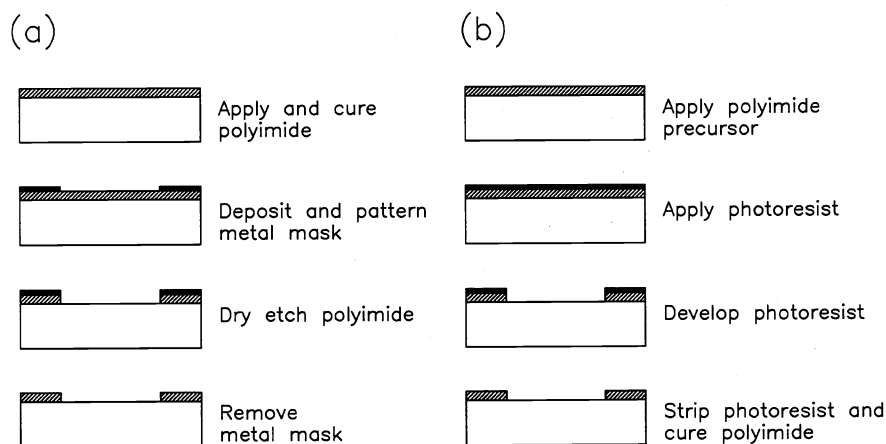


**Figure 2.1.1:** Processing of polyimide. (a) Patterning by dry etching. (b) Patterning by photolithography.

In principle two methods exist to pattern the polyimide layer<sup>7</sup>, shown in figure 2.1.1. After spinning on the precursor and removing the solvent by prebaking, the film can be cured immediately. However, after curing, the polyimide film becomes insoluble in virtually all chemicals. Only hot bases, and very strong acids will dissolve the material. Since masking against such chemicals is very difficult, dry etching by means of an oxygen plasma is normally applied. For this purpose, a metal mask must be deposited and patterned on top of the polyimide, and subsequently be removed after the patterning of the polyimide. A simpler method, shown in figure 2.1.1(b), is not to cure the precursor directly after spinning, but instead apply a photoresist layer on top. Since the precursor is dissolved in the basic photoresist developer, the pattern in the resist will be transferred directly to the polyimide during development of the photoresist. The photoresist may subsequently be stripped, using a chemical which does not dissolve the precursor (e.g. acetone), and the polyimide pattern can be formed by curing. The wet chemical etching is attractive because of its simplicity, however, since the patterning with the photoresist developer is difficult to control, the dry etching method offers higher resolution (typically 5 times), which is the reason why this method is preferred in the IC technology. The adhesion of the polyimide film on the underlying substrate is critical for the stability of the component containing the film, and has been investigated extensively in the literature<sup>7-10</sup>. It has been found that the adhesion on normally hydrolysed surfaces may be significantly improved by applying a silane based promoting agent to the substrate immediately before spinning of the polyimide precursor. This surface treatment will improve the adhesion on surfaces such as silicon and derivatives (oxide, nitride, oxynitride), aluminium and copper, however, the adhesion still deteriorates over time. One of the few materials where no deterioration of adhesion has been detected is chromium<sup>8-10</sup>. Furthermore, experiments have shown that no adhesion promotion is required on chromium surfaces<sup>9</sup>.

Another important polyimide technology, which has emerged is the application of photosensitive polyimides<sup>7,11</sup>. The precursor for this type of polyimide is derived in the same manner as described above, and is typically based on the PMDA-ODA synthesis. However, the carboxylic groups in the polyamic acid have been esterified with photoreactive acrylic-methacrylic groups. Upon illumination, these groups react, forming cross links of the polyamic acid, whereby it becomes insoluble. This way the polyimide precursor has acquired the properties of a negative photoresist, and may be processed using conventional lithography, and developed with one of the organic solvents mentioned above. During the imidisation of the polyimide precursor, the cross-linked photosensitive groups are depolymerised and expelled from the polymer. This additional cleavage compared to conventional polyimides cause the film to shrink somewhat more during imidisation, wherefore the resolution of photosensitive polyimides is inferior to polyimide. Considering, however, the processing of

photosensitive polyimide, it is clear that the fabrication of these layers is much more simple than the processes shown in figure 2.1.1. Commercial resins of photosensitive polyimide are available from a number of suppliers, such as OCG Microelectronics HTR 3 series, duPont® E38675-50, Ciba-Geigy Probimide™ 300 series, and Hitachi PL-1100.

## 2.2 Polyimide properties

As mentioned above, polyimide is today being used for passivation and insulation layers in the IC technology and hybrid packaging. Therefore, comprehensive research into the electrical and mechanical properties of polyimide films has been conducted.

### 2.2.1 Electrical properties

The electrical properties of polyimide are very essential in the IC technology, since they have direct influence on the performance of the circuit. The issues investigated include the dielectric constant, dielectric loss, and electrical breakdown and leakage. From these investigations a relative dielectric constant of 3.1-3.5 for PMDA-ODA polyimide has been reported. However, this value depends on the film thickness<sup>12</sup>, the temperature<sup>12</sup>, and the relative humidity<sup>9</sup>. An increase in any of these parameters will cause the dielectric constant to increase. Most significantly, changes of up to 35 % of the dielectric constant over the full relative humidity range has been reported<sup>9</sup>. For this reason, polyimide is also a suited material for humidity sensors. This dependence on humidity is explained by the adsorption of water molecules in the free space within the polymer. Since the relative dielectric constant of water is high ( $\epsilon_r \approx 80$ ), small amounts of water will influence the dielectric constant. Measurements have shown that a PMDA-ODA polyimide film will absorb between 2.5 % and 3.5 % of its own weight in water. The dissipation factor  $\tan \delta$ , which accounts for the dielectric loss in the film has been found to be  $0.7 \cdot 10^{-3}$  to  $3 \cdot 10^{-3}$  for the full relative humidity range<sup>9</sup>, and was found to be a function of the curing temperature of the polyimide<sup>13</sup>. It has been shown that a minimum of the dissipation factor occurs when the film is fully cured<sup>13</sup>. Further experiments show that the dissipation also is smaller if the polyimide is cured in nitrogen instead of air<sup>13</sup>. The breakdown electrical field has been measured to be between 3.3 MV/cm and 1.6 MV/cm for relative humidities between 0 % and 100 %<sup>9</sup>, and the resistivity was found to be depending on the curing conditions, film thickness, temperature, and field strength<sup>12</sup>. Typical resistivities measured at room temperature are in the range of  $10^{16} \Omega \text{cm}^{12}$ .

### 2.2.2 Mechanical properties

In the IC technology, the mechanical properties of the polyimide concern the stability of the component, and not directly the performance. However, if the material is to be used in a mechanical sensor, these properties will determine the performance of the sensor, and must consequently be known. Several authors have worked on this<sup>9,14,15</sup>, however, since these parameters depend on the exact polyimide resin and the preparation of the film, experiments are needed to determine the actual properties.

The intrinsic stress in the polyimide film is generated due to the mismatch of the coefficient of thermal expansion (CTE) between the film and the substrate. Since the CTE of polyimide can be as high as 50 ppm/°C<sup>14</sup>, compared to 3 ppm/°C for silicon, a tensile intrinsic stress appears in the film when it is cooled from the curing temperature ( $\geq 300$  °C). Furthermore, the chemical reaction (imidisation) and evaporation of solvent/photosensitive groups of the polymer causes a loss of volume, thereby adding to the intrinsic tensile stress. Substrate curvature experiments have been performed on 3 inch, 380  $\mu\text{m}$  thick silicon wafers, which were covered with a 1.5  $\mu\text{m}$  thick thermal silicon dioxide layer. A layer of the photosensitive polyimide precursor HTR3-200 from OCG Microelectronics was spun on to the wafer (3000 rpm, 20 s), and cured at 300 °C for 1 hr in a conventional convection oven. Before applying the precursor, a silane adhesion promoter  $\gamma$ -APS (aminopropyltriethoxysilane) was used to treat the silicon oxide surface. The average stress measured in the films was 33 MPa, which is in good agreement with previously published results giving values ranging from 30 MPa to 70 MPa. Furthermore, the stress was monitored over a period of 80 days (figure 2.2.1(left)), to determine the presence of relaxation phenomena. As it can be seen, the stress in the film decreases over time. However, no exact information about the relaxation can be obtained, since also the strain induced by the substrate decreases, as the deflection decreases. From the results, it seems that the stress of the polyimide tends to level off around a value of approximately 20 MPa. This is further supported by the measurements shown in figure 2.2.1(right), which were performed on a similar polyimide film, which was cured at 300 °C for 1 hr in a vacuum oven with 2 mbar N<sub>2</sub> applied. These data indicate that the stress relaxes quickly (within a few days) and remains stable at a specific level, which in this case was approximately 23 MPa.

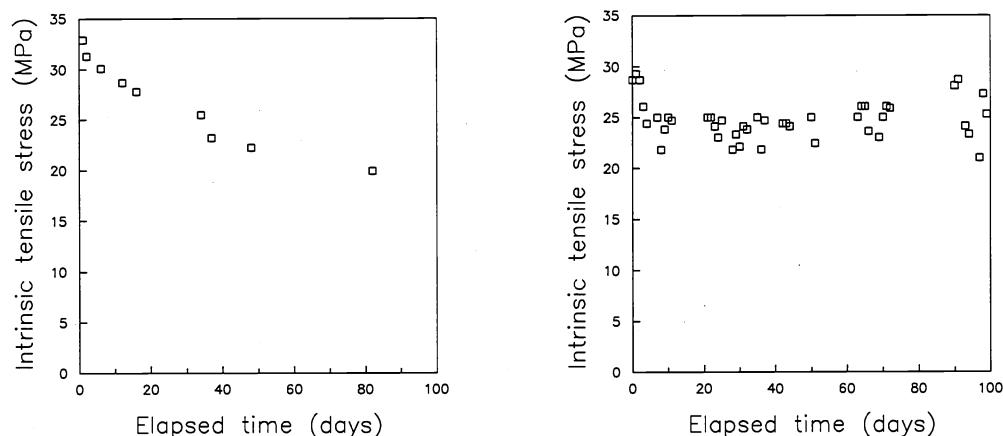


**Figure 2.2.1:** The average stress of HTR3 polyimide film vs. elapsed time. Left: Film cured in convection oven. Right: Film cured in 2 mbar N<sub>2</sub>.

The dynamic mechanical properties of the viscoelastic polyimide have been investigated by Pecht et al.<sup>16</sup> As expected for polymers, the Young's modulus was found to depend on the strain, the temperature, and the strain rate. Also the creep strain of the polyimide depends on the temperature and the stress level. However, since the glass transition temperature of polyimides is at least as high as the curing temperature ( $\geq 300^\circ\text{C}$ )<sup>14</sup>, these effects are expected to show little influence on the device operations at room temperature, since the effects are very slow (several days). Therefore, only the issue of long term stability regarding the intrinsic stress (figure 2.2.1) must be considered. This issue is best treated by keeping it in mind when evaluating the actual sensor devices, since these complex relaxation mechanisms will eventually depend on the complete structure containing the polyimide film(s).

The properties of polyimide are summarised in table 1, and for the purpose of comparison values for silicon and silicon nitride are also given. Comparing the intrinsic stress and the Young's modulus of the polyimide, it is clear that any micro-mechanical polyimide structure will be dominated by the stress. This means that the mechanical sensitivity of such structures will not directly be higher than for silicon nitride structures. However, since the density of the polyimide is much lower, larger structures may be made without problems with resonances arising, thereby increasing the mechanical sensitivity. From these results it must be concluded that the use of polyimide in mechanical sensors may be favourable if the properties can be controlled. Furthermore, new (photosensitive) polyimides with thermal expansion properties closely matched to silicon are being developed<sup>17</sup>, and therefore it is believed that polyimide layers with lower stress levels, and higher mechanical sensitivities can be made in the future.

**Table 1: Properties of polyimide**

	Polyimide	Silicon (110)	Silicon nitride
Dielectric constant	3.1-3.5	11.7-12	7-10
Dissipation factor ( $\tan \delta$ )	$10^{-3}$	-	-
Breakdown electrical field	1.6-3.3 MV/cm	0.1 MV/cm	1-10 MV/cm
Resistivity	$10^{16} \Omega\text{cm}$	0.1-60 $\Omega\text{cm}$	$10^{12} \Omega\text{cm}$
CTE	50 ppm/ $^\circ\text{C}$	3 ppm/ $^\circ\text{C}$	2.5-3 ppm/ $^\circ\text{C}$
Density	1430 kg/m <sup>3</sup>	2329 kg/m <sup>3</sup>	3400 kg/m <sup>3</sup>
Intrinsic stress	20-70 MPa	0	-50-100 MPa
Young's modulus	4-10 GPa	170 GPa	130 GPa
Poisson's ratio	0.45	0.066	0.2

### 3. APPLICATIONS IN CAPACITIVE SENSORS

For the fabrication of capacitive mechanical sensors in polyimide, a complete process module has been developed<sup>18</sup>. With this process different sensors may be fabricated simply by modifying the masks in the process, similar to the IC technology. The fabrication process, involving both surface and bulk micromachining, has been described in detail elsewhere<sup>19,20</sup> and will therefore only be briefly illustrated here.

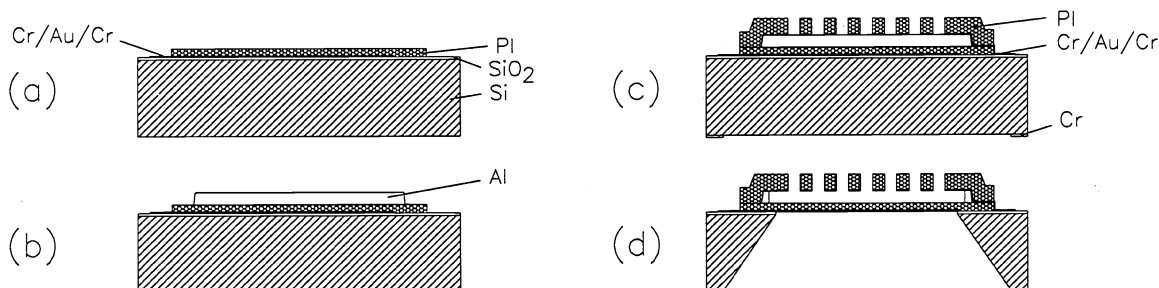


**Figure 3.1:** Polyimide sensor process. (a) Deposition of the first Cr/Au/Cr metal electrode and polyimide layer. (b) Deposition of Al sacrificial layer. (c) Deposition of the second Cr/Au/Cr metal electrode and polyimide layer, and deposition of Cr etch mask on the backside of the Si substrate. (d) Etching of Al sacrificial layer and Si substrate.

The process is carried out on silicon substrates covered with an insulating layer, such as thermal silicon oxide. In the event that the process is performed on substrates already containing integrated electronic circuitry, this layer will be present from the IC process. Firstly, a Cr/Au/Cr electrode layer is deposited and patterned using lift-off with photoresist, and the first PI layer is spun on, patterned and cured (figure 3.1(a)). All polyimide layers described in the following have been produced using the HTR3-200 photosensitive polyimide precursor from OCG Microelectronics Inc, in which different layer thicknesses have been realised by changing the spinning parameters and/or the viscosity of the precursor by additional solvent. After curing, the Al sacrificial layer is deposited and patterned (figure 3.1(b)), and the second Cr/Au/Cr electrode layer and polyimide layer are applied in a similar manner to the first layers. Subsequently, a Cr layer is deposited on the backside of the substrate, to serve as mask for the etching of the silicon substrate (figure 3.1(c)). Finally, the sacrificial layer is etched in a chemical solution containing phosphoric acid, and the silicon substrate is etched using dry reactive ion etching (RIE) with a gas composition of SF<sub>6</sub>/CHF<sub>3</sub>/O<sub>2</sub> (figure 3.1(d)). In the etching of the silicon substrate, the first Cr/Au/Cr electrode layer furthermore acts as an etchstop. The device shown in figure 3.1(d) has two metallised polyimide diaphragms, and was developed to be used as a condenser microphone, which is one of the three possible capacitive sensor applications described in the following.

#### 3.1 The polyimide condenser microphone

The desire to develop a condenser microphone with integrated signal detection circuit has been the background for the evolution of capacitive sensors in polyimide. The advantages of integrating a condenser microphone with the detection circuit is, as for all capacitive sensors, that the parasitic loading of the sensor can be minimised, together with a reduction of the induced noise. This improvement of the performance of the microphone is believed to make the micromachined devices competitive with the conventional technology of electret microphones for applications such as hearing aids. The use of condenser microphones, which are biased by an external DC voltage, may be favourable compared to electret microphones, as the issue of charge stability on the electret can be eliminated. Furthermore, the introduction of micromachining has made it possible to realise structures with air gaps between diaphragm and backplate in the order of a few microns compared >10 μm for conventional technologies. This has resulted in a significant reduction of the required DC bias voltage from >200 V to 5-20 V, which may be generated from a small battery with a DC-DC voltage converter circuit (a charge pump).

In figure 3.1.1, the cross-sectional view and a SEM photograph of a polyimide condenser microphone is shown. The condenser microphone is in principle a pressure sensor, sensitive to pressure variations down to ten orders of magnitude smaller than normal ambient pressures. The microphone basically consists of a diaphragm and a backplate, separated by an air gap. As the diaphragm moves according to the sound pressure variations, the acoustic holes in the backplate allow the air in the air gap to flow freely to and from the gap<sup>19</sup>. The number of holes in the backplate is related to the height of the air gap, and must be chosen large enough to minimise the viscous damping of the air flow, and thereby ensure a sufficiently high cut-off frequency of the microphone. The movement of the diaphragm, which results in a changing capacitance between

diaphragm and backplate, is normally detected by applying a static electrical field in the air gap and measuring the small variations of electrical potential over the microphone with an amplifier with very high input impedance.

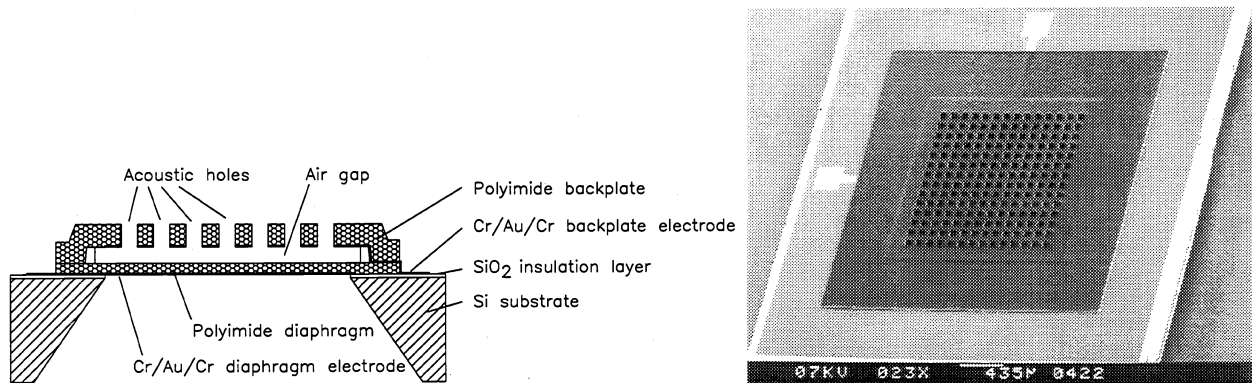


Figure 3.1.1: Cross-sectional view and SEM front view of the polyimide condenser microphone.

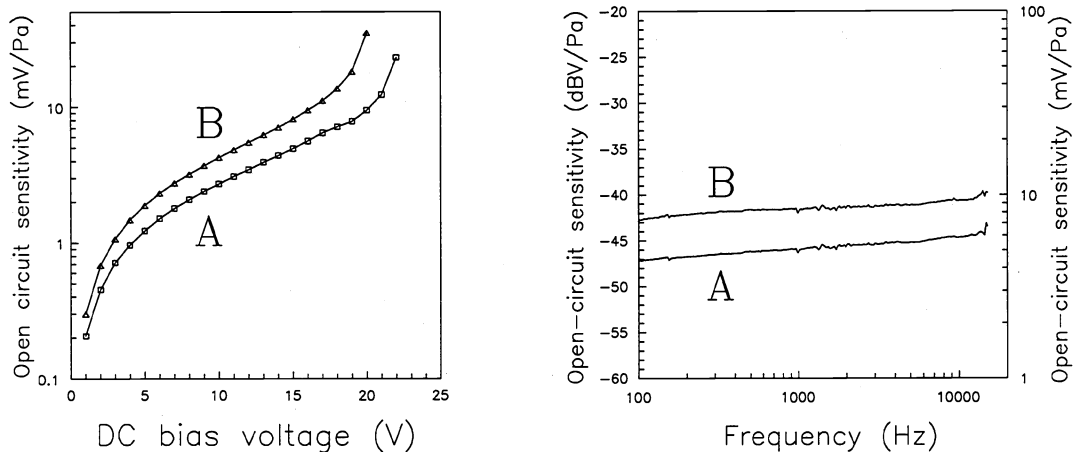


Figure 3.1.2: Measured characteristics of the polyimide condenser microphones. Left: Open-circuit sensitivity vs. DC bias voltage (frequency: 1 kHz). Right: Frequency response (DC bias voltage: 15 V). (A: 1.6 mm, B: 2.1 mm).

The microphone has been fabricated according to the process described above, in which the thickness of the diaphragm and the perforated backplate was  $0.9 \mu\text{m}$  and  $18 \mu\text{m}$ , respectively. The air gap was  $1.5 \mu\text{m}$ , and devices with diaphragm sizes of 1.6 mm (A) and 2.1 mm (B) were realised. The microphones have been tested in an acoustical measurement set-up, in which the frequency response and sensitivity can be obtained by comparison to that of a known Brüel & Kjær reference microphone<sup>21</sup>. The measured open-circuit sensitivity as function of the DC bias voltage and the frequency response of the two sizes of microphones are shown in figure 3.1.2. The measurements of the sensitivity vs. DC bias voltage (figure 3.1.2(left)) demonstrate the well known properties of stability of the condenser microphone. The characteristic curves, containing a linear, exponential, and over-exponential segment, illustrate the influence of the electrostatic attraction forces between the diaphragm and the backplate caused by the DC bias voltage. Above a certain level, known as the critical bias voltage (CBV), these forces cause a collapse of the structure. The CBV for the microphones was measured to be 23 V for (A) and 21 V for (B), and the values, together with the shape of the curves, were found to be in good agreement with theoretical analyses<sup>19</sup>. The frequency responses of the microphones, operated at a bias voltage of 15 V, were found to be flat ( $\pm 2$  dB) in the measured range between 100 Hz and 15 kHz. Furthermore, an open-circuit sensitivity of 5.1 mV/Pa (A) and 8.1 mV/Pa (B) was measured at 1 kHz, and the noise levels were determined to be 28 dB SPL (A) and 24 dB SPL (B).

### 3.2 The polyimide pressure sensor

The polyimide process technology can also be directly exploited to fabricate a capacitive pressure sensor (figure 3.2.1(left)). This structure can be realised by modifying the masks, whereby an opening is added in the first Cr/Au/Cr- and polyimide layer and the holes in the second polyimide layer are removed. In this situation, what was previously the thick polyimide backplate

in the microphone now acts as the sensing diaphragm in the pressure sensor. The opening in the silicon substrate has been reduced, such that the first polyimide layer only serves the purpose of electrical insulation.

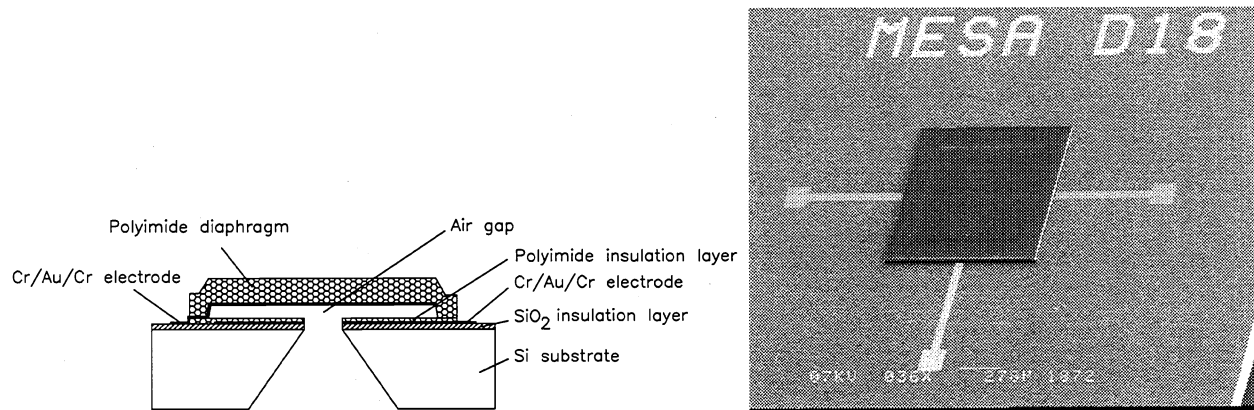


Figure 3.2.1: Cross-sectional view and SEM front view of the polyimide pressure sensor.

From theoretical considerations, concerning the deflection of the polyimide diaphragm, a sensor for a pressure range of 1 bar has been designed and fabricated<sup>20</sup>. The SEM photograph in figure 3.2.1 depicts the front of the device, showing the polyimide diaphragm and the electrical connections. The size and the thickness of the diaphragm was chosen to be  $700 \times 700 \mu\text{m}$  and  $15 \mu\text{m}$ , and the height air gap was  $5 \mu\text{m}$  and the thickness of the first polyimide insulation layer was  $0.5 \mu\text{m}$ . These dimensions yield a theoretical centre deflection of  $3.6 \mu\text{m}$  of the diaphragm for a pressure of 1 bar, and a sensor capacitance of  $0.62 \text{ pF}$  with no pressure applied. The theoretical relation between the sensor capacitance and the applied pressure difference is shown in figure 3.2.2 (left). As can be seen, a relative change of  $0.14 \text{ pF}$  (22 %) of the capacitance is expected in the range 0-1 bar.

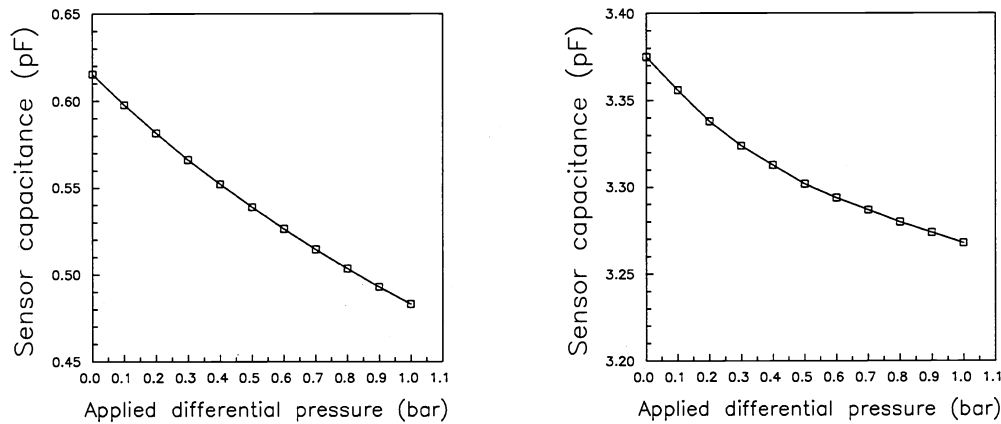


Figure 3.2.2: Calculated (left) and measured (right) capacitance of the pressure sensor vs. applied differential pressure.

The sensor chip was mounted on a printed circuit board and tested in a set-up where the pressure can be applied to backside of the device. The capacitance of the sensor was monitored with an HP 4194A Impedance Analyzer, and the resulting measurements are shown in figure 3.2.2(right). It appears that the measurements are somewhat different from the theory, as the relative change  $\Delta C/C$  is only 3.2 %. This can be explained by the parasitic capacitance of the connections between the sensor and the analyzer, causing also the high value of the measured sensor capacitance. Subtracting a parallel parasitic capacitance of  $2.7 \text{ pF}$  from the measurements yields a relative change  $\Delta C/C$  of 17%, which is in good agreement with the theory. This result illustrates well the importance of minimisation of the parasitic effects in capacitive sensors.

### 3.3 The polyimide uni-axial accelerometer

A third possibility of the fabrication process is to produce a capacitive accelerometer (figure 3.3.1). Since the viscoelastic polymer material can absorb much larger energies than solids at high strain rates (shocks) without breakage, this

accelerometer could be useful in applications that must be resistant to very large shocks. The fabrication of this device is simpler than the previous examples, since no etching of the silicon substrate is required in this purely surface micromachined structure. As for the pressure sensor, the first Cr/Au/Cr- and polyimide layer serves respectively as fixed counter electrode and electrical insulation layer. The device consists of a seismic mass, in form of a polyimide plate, suspended diagonally on four polyimide beams. All of which are realised in the second Cr/Au/Cr- and polyimide layers.

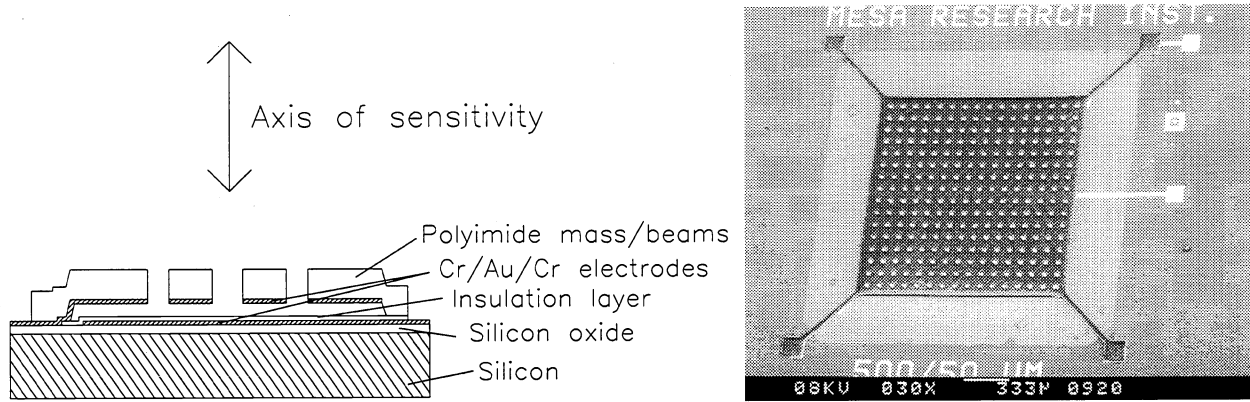


Figure 3.3.1: Cross-sectional view and SEM front view of the polyimide accelerometer.

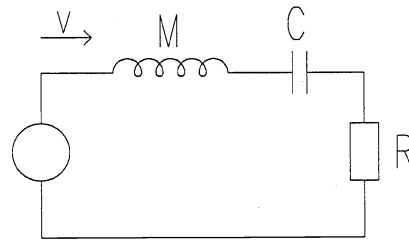


Figure 3.3.2: Mechanical equivalent circuit of the accelerometer.

In operation, the external force exerted on free structure will cause it to deflect, and as the beam suspension is much more compliant than the plate (mass) itself, it can be assumed that the plate experience a piston-form movement. The dynamic mechanical behaviour can be described with the linear circuit shown in figure 3.3.2. In this equivalent mechanical circuit, the source  $F$  represents the force applied to the seismic mass, the coil  $M$  the inertia of the seismic mass, the capacitor  $C$  the compliance of the four beam suspensions, and the resistor  $R$  the damping caused by air flowing in the thin air gap between the seismic mass and the substrate. The value of the components for the structure shown in figure 3.3.1 are given by:

$$M = \left(1 - \frac{4a^2}{b^2}\right) L^2 (h\rho + h_e\rho_e) \quad F = Ma \quad (1)$$

$$C = \left(\frac{4EW_{beams}h^3}{L_{beams}^3} + \frac{4\sigma W_{beams}h}{L_{beams}}\right)^{-1} \quad R = \frac{1.22\eta\pi L^2 b^2}{h_a^3} B$$

where  $2a$  and  $b$  are the size and centre-to-centre distance of the holes in the plate,  $L$  and  $h$  are the size and the thickness of the polyimide plate and beams,  $\rho$  and  $E$  are the density and Young's modulus of polyimide,  $h_e$  and  $\rho_e$  are the thickness and the density of the second Cr/Au/Cr layer,  $\sigma$  is the intrinsic stress,  $W_{beams}$  and  $L_{beams}$  are the width and length of the polyimide beams,  $\eta$  is the dynamic viscosity of air ( $17.1 \mu\text{Pa s}$ ),  $h_a$  is the height of the air gap, and  $B$  is a value concerned with the position and size of the holes in the polyimide plate<sup>22</sup>:

$$B = \frac{1}{4} \ln\left(\frac{X_0^2}{R_h^2}\right) - \frac{3}{8} + \frac{1}{2} \frac{R_h^2}{X_0^2} - \frac{1}{8} \frac{R_h^4}{X_0^4} \quad (2)$$

$$X_0 = 0.565b \quad R_h = a\sqrt{2}$$

The flow (current)  $v$  in the equivalent circuit denotes the velocity of the seismic mass, and in the harmonic situation the amplitude of the movement may be derived simply by dividing the velocity by the angular frequency  $\omega$ . An accelerometer was designed and fabricated with the following dimensions:  $L$ : 2mm,  $h$ : 13 $\mu\text{m}$ ,  $2a$ : 40 $\mu\text{m}$ ,  $b$ : 80 $\mu\text{m}$ ,  $h_a$ : 2 $\mu\text{m}$ ,  $W_{\text{beams}}$ : 50 $\mu\text{m}$ ,  $L_{\text{beams}}$ : 500 $\mu\text{m}$ . A calculation of the equivalent circuit yields a mechanical sensitivity of 6.47 nm/g, corresponding to a nominal sensitivity  $\Delta C/C$  of 0.32 %/g. The accelerometer was mounted on a mechanical shaker and tested with an amplitude modulated (AM) detection circuit, shown in figure 3.3.3. The charge amplifier with the accelerometer  $C_{\text{sens}}$  and the feedback capacitor  $C_{\text{fb}}$  is operated at 200 kHz, and the bias resistor  $R_b$  is used prevent charging of the input. The 200 kHz carrier signal is then removed with the low-pass filter  $R_{\text{lp}}$  and  $C_{\text{lp}}$ , leaving an output signal  $v_{\text{out}}$  which is directly proportional to the change of the sensor capacitance.

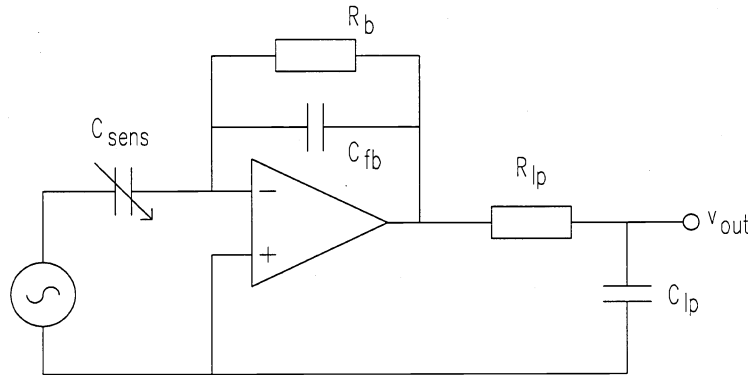


Figure 3.3.3 AM detection circuit for the accelerometer.

The applied acceleration was measured with a reference accelerometer, and the recorded change of capacitance  $\Delta C/C$  vs. the acceleration is shown in figure 3.3.4(left) for a frequency of 100 Hz. As can be seen, the measured sensitivity (0.43 %/g) is somewhat higher than the predicted value, however, the linearity in the measured range is still good. This implies that the compliance is higher in the realised devices. The frequency response of the accelerometer was measured in a range between 20 Hz and 3 kHz. In figure 3.3.4(right), the measured nominal sensitivity is shown together with simulated response derived from equations (1) and (2). For frequencies below 1 kHz, there is reasonable agreement between measurements and theory. The resonance peaks at higher frequencies are not believed to be caused by the sensor itself, but rather from insufficiently firm packaging of the sensor onto the shaker.

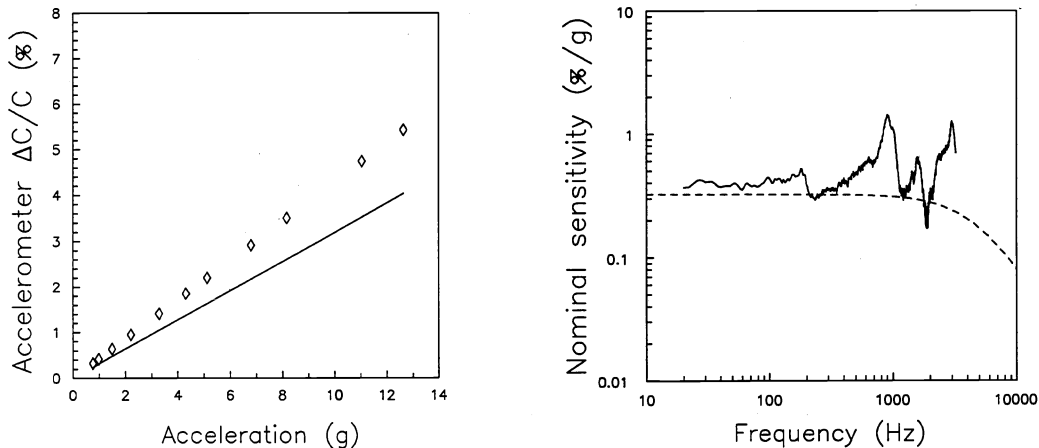


Figure 3.3.4: Change of capacitance vs. applied acceleration (Line: Theory.  $\diamond$ : Measurement), and frequency response (Dashed line: Theory. Solid line: Measurement) of the accelerometer.

#### 4. CONCLUSIONS AND DISCUSSION

In this paper a modular fabrication process for capacitive mechanical sensors has been suggested. The process was developed with the intention of achieving full integration of the sensor and the electronic signal conditioning circuitry in a simple and reliable manner, to fully exploit the high performance of capacitive sensors. The best solution to this complex problem is to develop a sensor process which can be performed independently of any IC process, thereby providing the best flexibility of the complete fabrication. The use of polymers in the sensor makes it possible to realise a fabrication process which is fully IC-compatible. One of the best suited polymers appears to be polyimide, as it is mechanically and chemically very stable and yet can be fabricated in a simple manner by spin coating and baking. Introduction of this material has resulted in a low-temperature (<300 °C) sensor fabrication process, which can be performed as a post-process directly on substrates containing integrated circuits.

Polyimide is a well characterised material, since it is used in IC processes and hybrid packaging as electrical insulation layer. Therefore, also a large variety of polyimide precursors are commercially available both with and without photosensitive properties. The structures described in this paper have all been made from one type of photosensitive polyimide (HTR3 from OCG Microelectronics), which can be applied in layers <1 µm to >50 µm. The three sensor applications illustrated in this paper serve to demonstrate how different device structures can be realised without changing the fabrication process, which adds to the flexibility of the process. From the results of the implemented sensor structures, it may be concluded that capacitive sensors with excellent properties can be produced with this process. There are however still issues to be concerned with, regarding long-term stability of polymers and structures based on them. For polyimide, no long-term degradation of properties is known to take place. Unfortunately, it is well known that polyimide absorbs water, leading to a change of the dielectric constant by up to 35 % over the full humidity range<sup>9</sup>. This may seem a significant change, however, for the structures shown in this paper only a thin film of polyimide is electrically involved in the sensor, and is always in series with the air gap. Therefore, as the sensor capacitance is largely determined by the air gap, calculations show that the influence of humidity will be <0.5 dB for the microphone and <1 % for the pressure sensor and the accelerometer, which in practice would be negligible. A more significant parameter is the thermal expansion, which for conventional polyimides is ≈16 times larger than silicon. For increasing temperatures, this leads to a reduction of the intrinsic stress in the polyimide film causing an increase of the mechanical sensitivity of the structures. Recent developments in polymer science seem to provide a solution to this problem, by the demonstration of new polyimide materials with thermal properties matched to silicon<sup>17,23</sup>. With the emerge of such new materials this leads to the conclusion that polymer processing may become a dominating fabrication method for smart sensors in the future, due to the simplicity and IC-compatibility.

#### ACKNOWLEDGEMENTS

The authors are indebted to Johan Bomer for the fabrication of the devices, Bert Otter for providing the SEM photographs, and to the Dutch Technical Foundation (STW) for the financial support.

#### REFERENCES

1. K. Petersen, "Silicon as a mechanical material", *Proc. IEEE*, **70**(5), pp. 420-457, 1982.
2. S. Middelhoek and A.C. Hoogerwerf, "Smart sensors: When and where?", *Sensors and Actuators*, **8**, pp. 39-48, 1985.
3. W. Kuehnel and S. Sherman, "A surface micromachined silicon accelerometer with on-chip detection circuitry", *Sensors and Actuators A*, **45**, pp. 7-16, 1994.
4. S.M. Sze, *Semiconductor devices, physics and technology*, p. 367, Wiley, New York, 1985.
5. S. Fang and J.P. McVittie, "Thin-oxide damage from gate charging during plasma processing", *IEEE Electron Dev. Lett.*, **13**, pp. 288-290, 1992.
6. Y.K. Lee and J.D. Craig, "Polymer materials for electronic applications", *ACS Symposium series*, **184**, p. 107, 1982.
7. D.S. Soane, *Polymers in microelectronics: fundamentals and applications*, Elsevier, Amsterdam, the Netherlands, 1989.
8. N.J. Chou, D.W. Dong, J. Kim and A.C. Liu, "An XPS and TEM study of intrinsic adhesion between polyimide and Cr films", *J. Electrochem. Soc.*, **131**, pp. 2335-2340, 1984.
9. R.J. Jensen, J.P. Cummings and H. Vora, "Copper/polyimide materials for high performance packaging", *IEEE Trans. Comp. Hyb. Manufact. Technol.*, **CHMT-7**, pp. 384-393, 1984.
10. D.L. Pappas, J.J. Cuomo and K.G. Sachdev, "Studies of adhesion of metal films to polyimide", *J. Vac. Sci. Tech. A*, **9**, pp. 2704-2708, 1991.

11. P.G. Rickerl, J.G. Stephanie and P. Slota, "Processing of photosensitive polyimides for packaging applications", *IEEE Trans. Comp. Hyb. Manufact. Technol.*, **CHMT-12**, pp. 690-694, 1987.
12. A.M. Wilson, "Polyimide insulators for multilevel interconnections", *Thin Solid Films*, **83**, pp. 145-163, 1981.
13. L.B. Rothman, "Properties of thin polyimide films", *J. Electrochem. Soc.*, **127**, pp. 2216-2220, 1980.
14. C. Goldsmith, P. Geldermans, F. Bedetti and G.A. Walker, "Measurements of stresses generated in cured polyimide films", *J. Vac. Soc. Tech. A*, **1**, pp. 407-409, 1983.
15. M. Mehregany, R.T. Howe and S.D. Senturia, "Novel microstructures for the in situ measurement of residual stress", *J. App. Phys.*, **62**, pp. 3579-3584, 1987.
16. M. Pecht and X. Wu, "Characterization of polyimides used in high density interconnections", *IEEE Trans. Comp. Hyb. Manufact. Technol. B*, **17**, pp. 632-639, 1994.
17. O. Rohde, P. Smolka, P.A. Falcigno and J. Pfeifer, "Novel auto-photosensitive polyimides with tailored properties", *Polymer Eng. Sci.*, **32**, pp. 1623-1629, 1992.
18. Patent application no. 1001733, Rijswijk, the Netherlands, November, 1995.
19. M. Pedersen, W. Olthuis and P. Bergveld, "A silicon condenser microphone with polyimide diaphragm and backplate", *Submitted for publication in Sensors and Actuators A*.
20. M. Pedersen, M.G.H. Meijerink, W. Olthuis and P. Bergveld, "An IC-compatible polyimide pressure sensor with capacitive readout", *Submitted for publication in Sensors and Actuators A*.
21. M. Pedersen, R. Schellin, W. Olthuis and P. Bergveld, "Electro-acoustical measurements of silicon microphones on wafer scale", *Accepted for publication in J. Acoust. Soc. Am.*
22. Z. Skvor, "On the acoustical resistance due to viscous losses in the air gap of electrostatic transducers", *ACUSTICA*, **19**, pp. 295-299, 1967/68.
23. A.E. Nader, K. Imai, J. Craig, C.N. Lazaridis, D.O. Murray III, M.T. Pottiger, S.A. Dombchik and W.J. Lautenberger, "Synthesis and characterization of a low stress photosensitive polyimide", *Polymer Eng. Sci.*, **32**, pp. 1613-1617, 1992.